Shape of the Cu 2p core level photoemission spectrum for monovalent, divalent and trivalent Cu compounds



1992 J. Phys.: Condens. Matter 4 2801

(http://iopscience.iop.org/0953-8984/4/11/009)

J. Phys.: Condens. Matter 4 (1992) 2801–2816. Printed in the UK

# Shape of the Cu 2p core level photoemission spectrum for monovalent, divalent and trivalent Cu compounds

K Karlsson†, O Gunnarsson and O Jepsen

Max-Planck Institut für Festkörperforschung, D-7000 Stuttgart 80, Federal Republic of Germany

Received 18 October 1991

**Abstract.** We calculate the shape of the 2p core level photoemission spectrum for $Cu_2O$, CuO and $NaCuO_2$, where Cu is formally mono-, di- and trivalent, respectively. Although the number of 3d electrons is similar in the three compounds, there is a large variation in the strength of the $d^9$-like satellite and in the width of the main line. We relate the differences between $Cu_2O$ and CuO to the difference in the valence, while for $NaCuO_2$ the detailed form of the hopping matrix elements is also found to be important.

## 1. Introduction

The Cu 2p core level photoemission spectrum shows some quite pronounced and interesting changes between $Cu_2O$ and CuO, where Cu is monovalent and divalent, respectively. In CuO there is a pronounced satellite at about 10 eV higher binding energy than the main peak, with the satellite having about half the weight of the main peak. In $Cu_2O$, on the other hand, this satellite has little or no weight. In CuO the main peak has a substantial broadening, while in $Cu_2O$ the width can be explained as lifetime broadening and instrumental resolution. $NaCuO_2$, where Cu is trivalent, is intermediate between CuO and $Cu_2O$, both in terms of peak width and in terms of the weight of the satellite. The aim of this paper is to study these differences.

The difference between CuO and $Cu_2O$ in terms of the satellite is usually explained as follows. In CuO, where Cu is divalent, the ground state has essentially $d^9$ character. When a core hole is created, the strong attractive potential from the core hole makes the $d^{10}$ configuration lower in energy than the $d^9$ configuration. Thus the leading peak in the core spectrum corresponds mainly to final states of $d^{10}$ character. However, since the ground state has mainly $d^9$ character, there is a strong coupling to final states with $d^9$ character, which leads to a satellite at larger binding energy. In $Cu_2O$, on the other hand, it is argued, the ground state has mainly $d^{10}$ character, and a $d^9$ satellite should have very little weight. This type of mechanism for a core level satellite was first proposed for Ni compounds by Kotani and Toyozawa [1]. In a recent paper [2] we have performed electronic structure calculations for $Cu_2O$, CuO and $NaCuO_2$. In these calculations we found that there is about 9.30 and 9.13 3d electrons in $Cu_2O$ and CuO, respectively. While the assignment of the absolute number of 3d electrons is somewhat ambiguous, we believe that the calculated difference between

† Present address: Physics Department, Chalmers University of Technology, S-412 96 Göteborg, Sweden.

0953-8984/92/112801+16$04.50  

the compounds should be reasonable. The small difference in the 3d occupancy is also supported by the chemical shift of the Cu 2p level, which only differs by about 1 eV between $Cu_2O$ and CuO [3]. Since the screened Coulomb integral between a core hole and a 3d electron should be of the order 10 eV, we do not believe that there could be a large difference (of the order 1) in the number of 3d electrons between $Cu_2O$ and CuO. This, however, means that the traditional explanation of the difference in satellite structure between $Cu_2O$ and CuO given earlier could not be completely correct. Here we want to show that the differences between $Cu_2O$ and CuO in terms of the strength of the satellite and the width of the leading peak can nevertheless be related to the difference in valence. The core level photoemission spectrum for divalent Cu has been studied by several groups before, [4, 5] but these studies did not address these issues.

In section 2 we discuss the method for calculating the spectra. In section 3 we present the results and trace the origin of the differences between the three compounds.

## 2. Method

We use the impurity Anderson model for describing the spectra. In this model we include explicitly the 3d level on the Cu atom where the core hole is made, while all other 3d levels are only included implicitly, as discussed later. This is expected to be a reasonable approximation for core spectra, which samples the local properties of the system. The Anderson model is given by

$$H = \sum_{\nu}(\tilde{\varepsilon}_d - U_c(1-n_c))n_\nu + \int \varepsilon n_{\varepsilon\nu}\,d\varepsilon + \int d\varepsilon\,(V_\nu(\varepsilon)\psi^\dagger_{\varepsilon\nu}\psi_\nu + \text{HC}) + U\sum_{\nu<\mu} n_\nu n_\mu + \varepsilon_c n_c \qquad (1)$$

where $\tilde{\varepsilon}_d$ is the energy of the 3d-level on the impurity site. The 3d states are labelled by an orbital index $m$ and a spin index $\sigma$, and $\nu = (m, \sigma)$ is a combined index. The index $\nu$ runs between 1 and $N_d = 10$. If a core hole is created ($n_c = 0$) the 3d level is lowered by $U_c$. The delocalized electrons are described by the second term. The hopping between the conduction states and the 3d state is described by the third term, where $V_\nu(\varepsilon)$ is a hopping matrix element. $U$ describes the Coulomb interaction between the 3d electrons. All multiplet effects have been neglected. Finally $\varepsilon_c$ gives the energy of the core level, which is assumed to be non-degenerate to simplify the notation.

We use a variational method applied earlier to Ce compounds [6]. In this method we introduce a many-electron basis set and express the ground state as a linear combination of these basis states. The basis states are illustrated in figure 1. For $Cu_2O$ we start with a basis state where both the 3d level and the conduction band are full. The structure of this basis set is dictated by electron counting, which also determines the Cu valence. In the next state (b in figure 1(*a*)) a 3d electron has hopped into the conduction band. This type of states must be important, since we know that the number of 3d electrons in the ground state should be substantially smaller than 10. We must also include states with two 3d holes, although the energy of these states should be appreciably higher than that for the $d^9$ and $d^{10}$ states. The

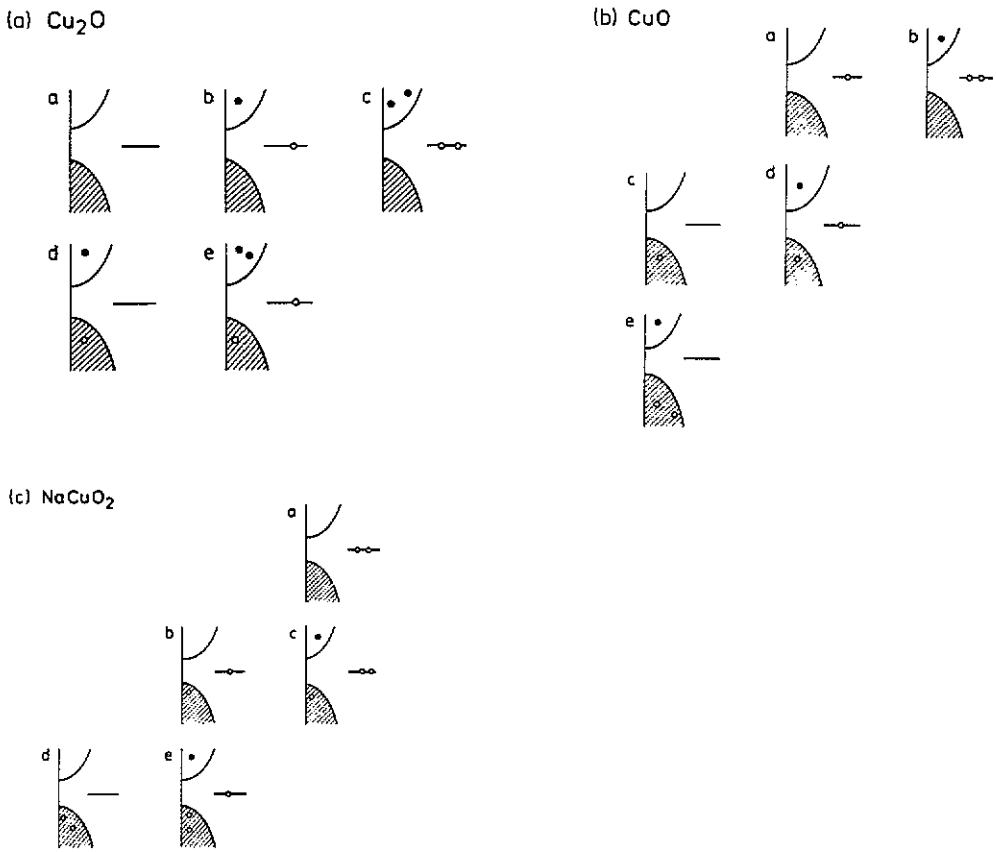


**Figure 1.** Basis states for $Cu_2O$ (*a*), CuO (*b*) and $NaCuO_2$ (*c*). The left column shows $d^{10}$ states, the middle $d^9$ states and the right $d^8$ states. The coupling is of the order $(1/N_d)^0$ within each row and of the order $(1/N_d)^1$ between two neighbouring rows.

reason is that the $d^8$ states push down the $d^9$ states, leading to a reasonable Cu 3d charge in the ground state. We next include states (d in figure 1(*a*)) which couple to the states b via the hopping of a valence electron into the 3d level. We finally add states (e in figure 1(*a*)) where an additional 3d electron has hopped into the conduction band.

In the Ce calculations it was very useful to introduce the inverse of the degeneracy of the localized level as a small parameter. If the hopping matrix elements $V_\nu(\varepsilon)$ are independent of the index $\nu$ we can follow this approach here too. We then consider a model where the degeneracy of the 3d level $N_d$ is formally considered as a parameter, although it will be given its physical value ($N_d=10$) at the end. We further let $V_\nu$ depend on $N_d$ in such a way that

$$\sqrt{N_d}V_\nu(\varepsilon) \equiv \tilde{V}(\varepsilon) \tag{2}$$

independently of $N_d$. As we shall see later, the coupling between states in the same row in figure 1 is then of zeroth order in $1/N_d$, while the hopping between states in two neighbouring rows is of the order $(1/N_d)^1$. To order $(1/N_d)^0$ it is then sufficient to consider the states a, b and c in figure 1(*a*).

We next consider the basis states for CuO in figure 1(*b*). We start with a state with a 3d hole and a filled valence band. This choice is again determined by the valence of Cu, which requires the 3d level or the valence band to have a hole. This state couples to the state b with two 3d holes. There is a further coupling to the state c with a valence hole and a filled 3d level. We expect the states a and c to be most important for the calculation. In contrast to $Cu_2O$, however, the coupling between these two states with $3d^9$ and $3d^{10}$ character is of order $(1/N_d)^1$, while in figure 1(*a*) the coupling between the states a and b is of the order $(1/N_d)^0$. We shall see later that this difference is important. We further include the states d and e with one conduction electron and one or two valence holes.

For $NaCuO_2$ we start with the state a containing two 3d holes and a full valence band, consistent with the valence 3 of Cu in this compound. This state has a high energy, and we expect states with $3d^9$ and $3d^{10}$ character to dominate the ground state. Thus we include the states b and d which have $d^9$ and $d^{10}$ character, respectively. However, we observe that the coupling between these states is of the order $(1/N_d)^1$. We therefore also include the states c and e which have a coupling of the order $(1/N_d)^0$ to the states b and d, respectively.

We now show more in detail how the basis states are defined and calculate the matrix elements between these states. We introduce the state a in figure 1(*a*) as

$$|d^{10}\rangle \tag{3}$$

where all the 3d and the valence levels are filled. The state b is defined as

$$|E\rangle = \frac{1}{V(E)\sqrt{N_d}} \sum_\nu V_\nu(E) \psi^\dagger_{E\nu} \psi_\nu |d^{10}\rangle \tag{4}$$

where

$$N_d V(E)^2 = \sum_\nu |V_\nu(E)|^2. \tag{5}$$

If $V_\nu$ is independent of $\nu$ we have $V(E) = V_\nu(E)$. The state $|E\rangle$ in (4) is normalized. The linear combination of the states in equation (4) is only one of $N_d$ different combinations. The state $|E\rangle$ is, however, chosen in such a way that all states which are orthogonal to $|E\rangle$ do not couple to $|d^{10}\rangle$ via the Hamiltonian. We then introduce a state

$$|E\varepsilon\rangle = \frac{1}{v(E,\varepsilon)\sqrt{N_d}} \sum_\nu V_\nu(E) V_\nu(\varepsilon) \psi^\dagger_{E\nu} \psi_{\varepsilon\nu} |d^{10}\rangle \tag{6}$$

where

$$N_d v(E,\varepsilon)^2 = \sum_\nu |V_\nu(E)|^2 |V_\nu(\varepsilon)|^2. \tag{7}$$

Here $v(E,\varepsilon) = V_\nu(E)V_\nu(\varepsilon)$ if $V_\nu$ is independent of $\nu$. $E$ indicates an energy in the conduction band and $\varepsilon$ an energy in the valence band. The state $|E\varepsilon\rangle$ is chosen in such a way that no other state with a conduction electron and a valence hole

orthogonal to $|E\varepsilon\rangle$ couples to $|E\rangle$. We note, however, that we can construct other states of the type b in figure 1(*a*), which couple to $|E\varepsilon\rangle$. We introduce a state

$$|\tilde{E}\rangle = \sum_{\nu} V_\nu(E)|V_\nu(\varepsilon_0)|^2 \psi^\dagger_{E\nu}\psi_\nu|\mathrm{d}^{10}\rangle. \tag{8}$$

This state is then orthogonalized to the state $|E\rangle$ and normalized, giving a new state $|E1\rangle$. This state does not couple to $|\mathrm{d}^{10}\rangle$ but in general it has a coupling to $|E\varepsilon\rangle$. The energy $\varepsilon_0$ in equation (8) is chosen to be an energy for which the state $|E\varepsilon\rangle$ has a large weight. If $V_\nu(\varepsilon) \equiv w_\nu f(\varepsilon)$, the states $|E\rangle$ and $|E1\rangle$ are the only ones coupling to $|E\varepsilon\rangle$, otherwise additional states can be constructed. If $|V_\nu(\varepsilon)|^2$ is independent of $\nu$, the state $|\tilde{E}\rangle$ is identical to $|E\rangle$ apart from a normalization constant, and no new state $|E1\rangle$ can be formed. In practice it turns out that $|E1\rangle$ plays an unimportant role. We finally form $\mathrm{d}^9$ states with two conduction electrons and one valence hole. We introduce

$$|EE'\varepsilon 1\rangle = \frac{1}{w_1(E,E',\varepsilon)\sqrt{N_\mathrm{d}(N_\mathrm{d}-1)}} \times \sum_{\nu\neq\nu'} V_\nu(E)V_{\nu'}(E')V_\nu(\varepsilon)\psi^\dagger_{E\nu}\psi_{\varepsilon\nu}\psi^\dagger_{E'\nu'}\psi_{\nu'}|\mathrm{d}^{10}\rangle \tag{9}$$

and

$$|EE'\varepsilon 2\rangle = \frac{1}{w_2(E,E',\varepsilon)\sqrt{N_\mathrm{d}}} \sum_{\nu} V_\nu(E)V_\nu(E')V_\nu(\varepsilon)\psi^\dagger_{E\nu}\psi_{\varepsilon\nu}\psi^\dagger_{E'\nu}\psi_\nu|\mathrm{d}^{10}\rangle \tag{10}$$

where we have introduced

$$N_\mathrm{d}(N_\mathrm{d}-1)w_1(E,E',\varepsilon) = \sum_{\nu\neq\mu} V_\nu(E)^2 V_\mu(E')^2 V_\nu(\varepsilon)^2 \tag{11}$$

and

$$N_\mathrm{d} w_2(E,E',\varepsilon) = \sum_{\nu} V_\nu(E)^2 V_\nu(E')^2 V_\nu(\varepsilon)^2. \tag{12}$$

For the states $|EE'\varepsilon 2\rangle$ we introduce the constraint $E \leqslant E'$, since $|EE'\varepsilon 2\rangle = -|E'E\varepsilon 2\rangle$. We next calculate the matrix elements of the Hamiltonian between these states. We obtain

$$\langle E|H|\mathrm{d}^{10}\rangle = \sqrt{N_\mathrm{d}}V(E) \tag{13}$$

$$\langle E\varepsilon|H|E'\rangle = -\frac{v(E,\varepsilon)}{V(E)}\delta(E-E') \tag{14}$$

$$\langle EE'\varepsilon 1|H|E_1\varepsilon_1\rangle = \sqrt{N_\mathrm{d}-1}\frac{w_1(E,E',\varepsilon)}{v(E,\varepsilon)}\delta(E-E_1)\delta(\varepsilon-\varepsilon_1) \tag{15}$$

and

$$\langle EE'\varepsilon 2|H|E_1\varepsilon_1\rangle = \left[\frac{w_2(E,E'\varepsilon)}{v(E,\varepsilon)}\delta(E-E_1) - \frac{w_2(E,E',\varepsilon)}{v(E',\varepsilon)}\delta(E'-E_1)\right] \times \delta(\varepsilon-\varepsilon_1). \tag{16}$$

If $V_\nu(E)$ is independent of $\nu$, it follows from equations (2), (5) and (15) that the matrix element between the states a and b in figure 1(*a*) goes as $\tilde{V}(E)$. From (2), (5), (7) and (14) it further follows that the coupling between the states b and d is of the order $(\tilde{V}(\varepsilon)/\sqrt{N_d})$. The matrix element (15) is of the order $\tilde{V}(E)$ while the element (16) is of the order $\tilde{V}(E)/\sqrt{N_d}$. Thus the leading matrix element between the states d and e is of the order $\tilde{V}(E)$. This illustrates the previous statement that the coupling between the states in a given row is of the order $(1/N_d)^0$, while the coupling (matrix element squared) between two states in neighbouring rows is of the order $(1/N_d)^1$. If we take into account that $V_\nu(E)$ depends on $\nu$ the difference between the coupling between states in the same row, on the one hand, and between states in different rows, on the other hand, is reduced. The extreme case is when we assume that only one 3d orbital with the label $m$ is of importance. Then only the spin degeneracy remains and we have effectively $N_d = 2$. Later we discuss more quantitatively where the real systems are located relative to these extreme limits.

The remaining states in figure 1(*a*) and the corresponding matrix elements can be obtained as earlier. The states for CuO and for $NaCuO_2$ can also be obtained in this way. For $NaCuO_2$ we assume the ground state to be a singlet state, i.e. we construct the states by starting with the state

$$|d^8\rangle = \psi_{x^2-y^2\uparrow}\psi_{x^2-y^2\downarrow}|d^{10}\rangle \tag{17}$$

where we have used the fact that the $x^2 - y^2$ orbital has the strongest coupling to the host and that this orbital therefore is empty.

The core-level spectra are now calculated as for Ce [6]. In the sudden approximation the core-level photoemission current is proportional to the core spectral function

$$\rho_c(\varepsilon) = \frac{1}{\pi}\,\mathrm{Im}\, g_c(\varepsilon - i0^+) \tag{18}$$

where

$$g_c(z) = \langle E_0|\psi_c^\dagger \frac{1}{z + H - E_0}\psi_c|E_0\rangle \tag{19}$$

$|E_0\rangle$ is the ground state and $\psi_c$ annihilates a core electron. Here, the Green function is calculated by formally assuming that the basis set used for the ground-state calculation is complete. We can then write

$$g_c(z) = \sum_{i,j}\langle E_0|\psi_c^\dagger|i\rangle\langle i|\frac{1}{z + H - E_0}|j\rangle\langle j|\psi_c|E_0\rangle \tag{20}$$

where $|i\rangle$ and $|j\rangle$ are the basis states used in the ground-state calculation but with the core level empty. Equation (20) can be evaluated by using the Lanczos method [7]. In this approach we transform to new basis states $|n\rangle$, which diagonalize $H(n_c = 0)$ in the space $\{|i\rangle\}$. Our spectra can then be written as

$$\rho_c(\varepsilon) = \sum_n |\langle n|\psi_c|E_0\rangle|^2\delta(\varepsilon - E_0 + E_n(N-1)) \tag{21}$$

where the final states $|n\rangle$ have the energies $E_n(N-1)$. In the sudden approximation this is the exact expression for the spectral function except for the use of the finite basis set.

The parameters of the model (1) have been determined from *ab initio* density functional [8, 9 (for a recent review.)] calculations using the local density (LD) approximation. Thus we calculate the hopping matrix elements using the formula [10]

$$|V_\nu(\varepsilon)|^2 = -\frac{1}{\pi}\,\mathrm{Im}\left[\int \mathrm{d}\varepsilon' \,\frac{\rho_\nu(\varepsilon')}{\varepsilon - \varepsilon' - \mathrm{i}0^+}\right]^{-1} \tag{22}$$

where $\rho_\nu(\varepsilon)$ is the projected 3d density of states (DOS) on a Cu atom. We have chosen the orbitals in such a way that in $Cu_2O$ the $3z^2 - 1$ orbital points in the direction of the two nearest neighbours and that the $x^2 - y^2$ orbital points towards the four nearest neighbours in CuO and $NaCuO_2$. The matrix elements in (22) have been obtained assuming that [10]

$$\sum_{\boldsymbol{k}} V^*_{\boldsymbol{k}m} V_{\boldsymbol{k}m'} \delta(\varepsilon - \varepsilon_{\boldsymbol{k}}) = |V_m(\varepsilon)|^2 \delta_{mm'} \tag{23}$$

where $\boldsymbol{k}$ labels the states in the electronic structure calculation, for example, is a combined index for a Bloch vector and a band index. $V_{\boldsymbol{k}m}$ is a matrix element between an extended state of the system and a localized 3d state with the orbital index $m$. In equation (23) it is assumed that the left-hand side is diagonal in $m$ and $m'$. This condition is only approximately satisfied in the present calculation. However, we find that the largest non-diagonal element in (23) is typically a factor 20 smaller than the diagonal elements.

The matrix elements have been adjusted for the configuration dependence [11]. Thus the ground-state matrix elements are scaled to correspond to the 3d occupancy 10, which is the appropriate one for the $d^9$ to $d^{10}$ hopping. For the final state we calculate the matrix elements in the presence of a core hole, which leads to a substantial reduction of the matrix elements [11]. The projected DOS $\rho_\nu(\varepsilon)$ has been calculated for a periodic solid, where the 3d levels on all Cu atoms couple to their surroundings. This method for obtaining the hopping matrix elements in the Anderson impurity model means that all the 3d levels in the compound are taken into account, although the 3d levels, which are not located on the impurity atom singled out in the Anderson impurity model, are treated in the LD approximation [10]. A drawback of this approach is that CuO is a metal in the LD approximation. Alternatively, in the LD calculation one can suppress the hopping from all 3d levels except the ones on the impurity atom and move the decoupled 3d levels above the Fermi energy. In this case CuO becomes an insulator, but all 3d levels except the ones on the impurity atom are completely neglected in the Anderson impurity calculation [10]. In view of the strong Cu 3d–O 2p coupling in these systems, we have used the first approach. Since the gap is too small or zero in the LD approximation, we have shifted the unoccupied states so that the experimental gap was obtained. The second approach gives qualitatively similar results, but the coupling to the valence band is somewhat stronger and more concentrated to the top of the valence band. For CuO this leads to a reduction in the satellite and to a narrower main peak.

We have also calculated the Coulomb integrals $U$ and $U_c$ as earlier [10]. Thus we perform super cell calculations with about 16 atoms, and vary the number of 3d electrons and core electrons to obtain $U$ and $U_c$. Thus we obtain $U$ from

$$U = \mathrm{d}\varepsilon_d / \mathrm{d}n_d$$

where $\epsilon_d$ is the 3d eigenvalue and $n_d$ is the 3d occupancy. In these calculations the hopping between the 3d level and the rest of the system has been suppressed, to avoid double counting of the hopping [10]. $U_c$ is obtained from

$$U_c = d\epsilon_d / dn_c$$

where $n_c$ is the occupation number of the core level. As previously, the hopping from the 3d level to the rest of the system has been suppressed. Finally we have also obtained, $\epsilon_d = \tilde{\epsilon}_d + 9U$, which is the energy difference between the $d^9$ and the lowest $d^{10}$ configuration. This difference is obtained as a transition state [12] calculation, by forcing the 3d occupation to be 9.5. The appropriate 3d occupation is obtained by applying an external field, and $\epsilon_d$ is given by the 3d eigenvalue.

The method for calculating the parameters combined with the Anderson impurity model has been tested for a number of system, both for spectroscopic properties [10, 13, 14] and thermodynamic properties [13]. The agreement with experiment is fairly good suggesting that the parameters are reasonable. Since each experimental property depends on several parameters in a complicated way, and since highly accurate solutions of the Anderson model have not yet been obtained for the 3d compounds, it is, however, not possible to estimate the errors in the calculated parameters.

The calculated spectra are given a Gaussian broadening of 0.7 eV full width at half maximum (FWHM). This broadening simulates the experimental resolution. We have further introduced a Lorentzian broadening of 1.1 eV (FWHM), to simulate the lifetime broadening. This broadening was chosen in such a way that the experimental broadening (1.4 eV) of the main peak for $Cu_2O$ is reproduced. The reason for this procedure is that the theory predicts that the main peak of $Cu_2O$ has a very small broadening due to electronic processes. This is in contrast to CuO where the theory predicts a large broadening. The Lorentzian broadening introduced for $Cu_2O$ may possibly also contain contributions from phonon broadening, although a Lorentzian is not well suited to describe such a broadening. The Lorentzian broadening we have introduced (1.1 eV) is somewhat larger than an experimental estimate ($0.72 \pm 0.17$ eV) of the lifetime broadening for Cu metal [15]. The lifetime broadening should be essentially the same for all Cu compounds, and the value introduced for $Cu_2O$ is therefore also used for CuO and $NaCuO_2$. In this way we have an effective test for whether or not the present model can describe the additional broadening observed for CuO and $NaCuO_2$.

## 3. Results and discussion

In figure 2 we illustrate the convergence of the calculation for CuO with the size of the basis set. The top of the figure shows the result using the basis states a and c in figure 1(*b*) (first-order). In a second-order calculation we also include the states b and d and in a third-order calculation the states e. The second- and third-order give practically identical results and only the third-order results are shown at the bottom of the figure. Because of the similarity between the second- and third-order results, we believe that the third-order results are well converged. The figure illustrates, however, that there is a substantial difference between the first- and third-order calculations. This is important to notice, since almost all calculations for CuO and the related high $T_c$ superconductors are performed using a first-order calculation. In the middle

of the figure we show results using a first-order calculation with the 3d level shifted 2.2 eV downwards. This curve agrees well with the third-order curve. A first-order calculation is therefore satisfactory for the core-level spectrum, if the 3d level position is treated as an adjustable parameter. If, however, the parameters are obtained from *ab initio* calculations, the first-order calculation is not sufficiently accurate. The reason is that in the second- and third-order calculations, the interaction with the states d in figure 1(*b*) lowers the $d^{10}$ configuration. The interaction with the states b at the same time lowers the $d^9$ configuration, but since the states b are high in energy, the effect on the $d^9$ configuration is smaller than for the $d^{10}$ configuration. The net result is a relative lowering of the $d^{10}$ configuration, which in a first-order calculation can be simulated by lowering the 3d level.

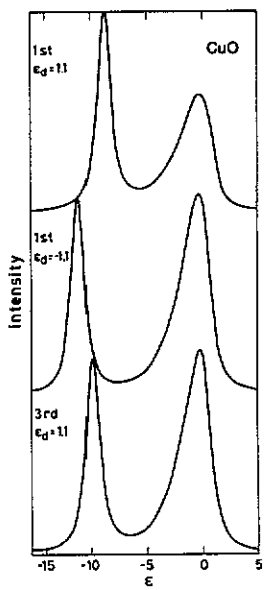


**Figure 2.** The spectrum for CuO using the states a and c in figure 1(*b*) (first-order) for two different values of the 3d level position ($\varepsilon_d$) and using the states a, b, c, d and e (third-order).

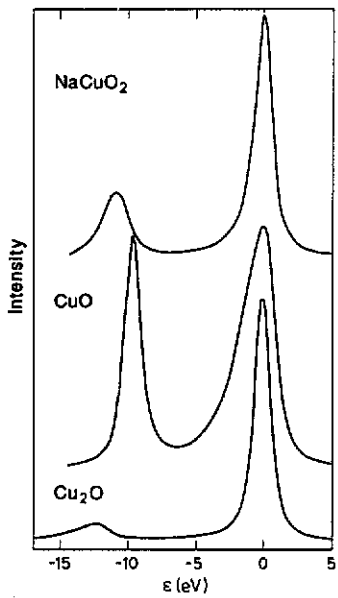


**Figure 3.** The 2p core spectra for $NaCuO_2$, CuO and $Cu_2O$. The absolute value of the energy is arbitrary and the main peaks have been lined up at zero. We have used the parameters $U = 8$ eV, $U_c = 10$ eV, and $\varepsilon_d = 2.3$ eV ($Cu_2O$), 1.1 eV (CuO) or 2.4 eV ($NaCuO_2$).

For $Cu_2O$ the first-order calculation (states a, b and c in figure 1(*a*)) gives well converged spectra but the $d^8$ states, as mentioned earlier, are important for achieving a reasonable Cu 3d charge. $NaCuO_2$ gives also converged spectra with just using the states a, b and d in figure 1(*c*).

In figure 3 we show the calculated Cu 2p spectrum for $Cu_2O$, CuO and $NaCuO_2$. The calculated values of $U$, $U_c$ and the hopping matrix element were used for all spectra. We have, however, adjusted $\varepsilon_d$ somewhat to get reasonable 3d occupancies, $n_d$, consistent with our earlier calculations [2]. We take $n_d = 9.42$, 9.25 and 9.24 for $Cu_2O$, CuO and $NaCuO_2$, respectively. These values are slightly larger than the ones from the *ab initio* calculations (9.30, 9.13 and 9.12), as is reasonable, since the *ab initio* values refer to the 3d charge inside a sphere with the Wigner–Seitz radius

$R_{WS} = 2.50\ a_0$ and since the true 3d orbital extends slightly beyond this sphere. We have, however, chosen $\varepsilon_d$ so that the difference in the 3d charge between the different compounds is the same as in the LD calculation. This is important, since the 3d charge strongly influences the weight of the satellite. For CuO our calculation leads to a local 3d spin moment of 0.57 $\mu_B$. This is to be compared with the experimental moment 0.65 $\mu_B$ [16]. A theoretical estimate [17] of the orbital component of the moment gave the value 0.13 $\mu_B$, suggesting the spin moment 0.52 $\mu_B$. Given that spin fluctuation should reduce the moment somewhat, our value (0.57 $\mu_B$) for the spin moment should be larger than the estimated experimental value (0.52 $\mu_B$). To obtain the quoted values for $n_d$ we raised the 3d level by 2.0, 0.5 and 2.1 eV for $Cu_2O$, CuO and $NaCuO_2$. Such an increase in the calculated value for the 3d level is reasonable, since the LD puts the 3d level about 1 eV too low in atomic total energy calculations [9]. As discussed later, an incomplete basis set can have the same effect as a shift of the 3d level. Another reason for the shift introduced for the 3d level, may therefore be that our basis set is not sufficiently complete.

The main peaks have been lined up at zero energy. These peaks have essentially $d^{10}$ character. The spectra also show satellites at about $-10$ to $-12$ eV. These satellites have mainly $d^9$ character. It is well established that these satellites have a substantial broadening because of multiplet effects [4]. Since no multiplet effects are included in the theory, the calculated satellites are much too narrow. The satellites may therefore appear to have too much weight compared with experiment. The experimental weights of the satellites relative to the main peaks are 0.55 and 0.2–0.4 for CuO and $NaCuO_2$, respectively. For $NaCuO_2$ the weight of the satellite is very uncertain due to the problems of separating the satellite from the background. For $Cu_2O$ it is not clear if the weight seen in the energy region where a satellite would be expected, really is a satellite of the type discussed here. Theoretically, the ratios of the satellite weight to the main peak weight are 0.19, 0.52 and 0.34 for $Cu_2O$, CuO and $NaCuO_2$, respectively, in satisfactory agreement with experiment. Thus we find that theory can account for the relative weights well. In particular, we find that the weight of the satellite for $Cu_2O$ is reduced substantially compared with CuO. Furthermore the satellite is broader for $Cu_2O$. This may be an additional important reason for the difficulties in seeing the satellite experimentally for $Cu_2O$. If, however, the satellite is seen at all for $Cu_2O$, it is shifted towards higher binding energies compared with CuO. This effect is also seen in the calculations. The shift is appearing due to the fact that in $Cu_2O$ the satellite contains mainly $d^9$ states with an electron in the conduction band. Due to the band gap these states are higher in energy by at least the gap compared to the satellite states in CuO which are pure $d^9$ states.

We can also see that the widths of the peaks are well described. Thus we find the widths 3.0 and 1.6 eV for CuO and $NaCuO_2$, respectively, compared with the experimental results 3.2 and 1.6 eV. As mentioned earlier, the Lorentzian broadening, describing core hole lifetime broadening, was adjusted so that the width (1.4 eV) of $Cu_2O$ was described correctly, since this should be the only essential intrinsic broadening mechanism for $Cu_2O$.

These results are not primarily due to peculiarities in the energy dependence of the matrix elements but due to the difference in states in figure 1 dictated by the difference in valence. To illustrate this we have performed calculations where the matrix elements calculated for $Cu_2O$ were used for CuO and *vice versa*. Since the strong coupling is in the $z^2$ symmetry for $Cu_2O$ but for $x^2 - y^2$ symmetry for CuO,

the $x^2 - y^2$ and $z^2$ symmetries were also exchanged. The result is shown in figure 4. We can see that the qualitative features of the spectra are not changed. For CuO there is an additional structure at about 5 eV higher binding energy than the main peak. This is due to a structure in the hopping matrix elements at this energy, and it disappears if the corresponding matrix elements are reduced. The width of the main peak (2.5 eV) is somewhat smaller than if the proper matrix elements are used (3.0 eV), but it is still much larger than for $Cu_2O$ (1.4 eV). The ratio of the weights of the satellite and the main peak is 0.47 which is only slightly smaller than the result (0.52) with the proper matrix elements. The $Cu_2O$ results in figure 4 are very similar to the results with proper matrix elements.

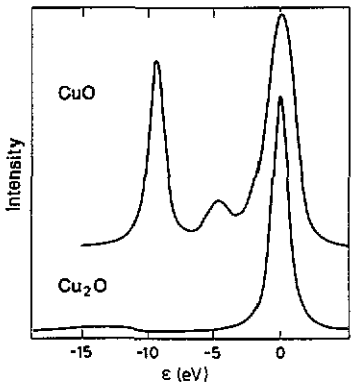


**Figure 4.** The core-level photoemission spectra for $Cu_2O$ and CuO using the matrix elements for CuO in the $Cu_2O$ calculation and *vice versa*.

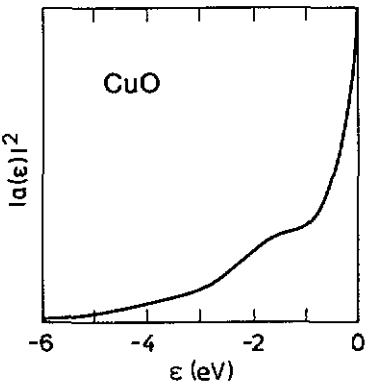


**Figure 5.** The coefficient $|a(\varepsilon)|^2$ in equation (26) as a function of the energy $\varepsilon$.

We first discuss the broadening of the main peak for CuO. To illustrate the origin we calculate the ground state including the states a and c in figure 1(*b*).

$$|E_0\rangle = A(\psi_\nu|\mathrm{d}^{10}\rangle + \int \mathrm{d}\varepsilon\, a(\varepsilon)\psi_{\varepsilon\nu}|\mathrm{d}^{10}\rangle) \tag{24}$$

where the first term gives state a and the second term the state c. $A$ and $a(\varepsilon)$ are variational coefficients and $\nu$ here refers to the state $x^2 - y^2$. We can solve for the energy lowering $\Delta E$ ($< 0$) relative to the energy $E_0^0$ of the $\mathrm{d}^9$ state

$$\Delta E = \int \mathrm{d}\varepsilon \frac{|V_\nu(\varepsilon)|^2}{\Delta E - \varepsilon_\mathrm{d} + \varepsilon}. \tag{25}$$

The coefficient $a(\varepsilon)$ can then be calculated as

$$|a(\varepsilon)|^2 = \frac{|V_\nu(\varepsilon)|^2}{|\Delta E - \varepsilon_\mathrm{d} + \varepsilon|^2} \tag{26}$$

i.e. the valence hole is spread out over an energy of the order $|\Delta E - \varepsilon_\mathrm{d}| \sim 4$ eV. The coefficient $a(\varepsilon)^2$ is shown in figure 5, and can be seen to have a broadening of the order 2–3 eV. In the presence of a core hole the $\mathrm{d}^{10}$ configuration is substantially

lower than the $d^9$ configuration. For the sake of the argument we therefore assume that the coupling between these configurations can be neglected. The final states are then pure $d^9$ states and $d^{10}$ states with a valence hole at the energy $\varepsilon$. The spectrum is determined by the coupling of these states to the ground state. Thus we obtain the spectrum

$$\rho_c(\varepsilon + \varepsilon_c + \Delta E - \varepsilon_d + 10U_c) = A^2[a(\varepsilon)^2\Theta(-\varepsilon) + \delta(\varepsilon - \varepsilon_d + U_c)] \tag{27}$$

where the first term corresponds to the main peak. In the present approximation, this peak obtains the same broadening as $a(\varepsilon)^2$. Together with the lifetime broadening and the instrumental resolution, the width of $a(\varepsilon)^2$ leads to the width of the main peak for CuO in figure 3. In $Cu_2O$, on the other hand, there is no valence hole for the lowest order $d^{10}$ configuration, and there is little broadening of the main peak.

For $NaCuO_2$ the main peak contains $d^{10}$ states with two holes in the valence band and we may expect a quite broad peak. The surprisingly narrow main peak is due to the very large hopping for $x^2 - y^2$ holes for energies close to the top of the valence band. To illustrate this, we have reduced the coupling by a factor of 10 for these energies, which makes the peak in $|V(\varepsilon)|^2$ and $|a(\varepsilon)|^2$ broader. This increased the width of the main peak by 0.8 eV. Thus the energy dependence of the hopping matrix $V_\nu(\varepsilon)$ is also important for the shape of the spectra.

We next discuss the small weight of the satellite in $Cu_2O$. As pointed out earlier, the satellite is broader for $Cu_2O$ than for CuO. The reason is that the $d^9$ configuration of $Cu_2O$ has a conduction electron, which is spread out over a certain energy interval. As for CuO we can solve for the ground state including the states a and b in figure 1(*a*). We then obtain the energy lowering $\Delta E$ relative to the $d^{10}$ state

$$\Delta E = N_d \int dE \, \frac{|V(E)|^2}{\Delta E - E + \varepsilon_d} \tag{28}$$

where $V(E)$ is defined in equation (5). Observe the factor $N_d$ in equation (28) compared with equation (25). The coefficient $b(E)$ of the $d^9$ states then has the form

$$|b(E)|^2 = N_d \frac{|V(E)|^2}{(\Delta E - E + \varepsilon_d)^2}. \tag{29}$$

Using the same type of arguments as earlier for CuO, we find that for $Cu_2O$ the satellite obtains a broadening determined by $|b(E)|^2$.

The broadening of the satellite for $Cu_2O$ makes it appear weaker, and harder to observe experimentally. However, the ratio of the weights of the satellite and the main peak (0.19) is also strongly reduced relative to CuO. We now discuss this. We use a simplified model with only one valence level for CuO and only one conduction level for $Cu_2O$. The ground state can then be written as

$$|E_0\rangle = a|d^9\rangle + \sqrt{1 - a^2}|d^{10}\rangle \tag{30}$$

where $a^2$ is the weight of the $d^9$ configuration. Here and in the following the core occupation is not shown explicitly. The final states are written as

$$|+\rangle = b|d^9\rangle + \sqrt{1 - b^2}|d^{10}\rangle \tag{31}$$

and

$$|-\rangle = \sqrt{1-b^2}|\mathrm{d}^9\rangle - b|\mathrm{d}^{10}\rangle \tag{32}$$

where $b^2$ is the weight of the $\mathrm{d}^9$ configuration in the lowest final state $|+\rangle$. The weight of the satellite is then

$$|\langle -|E_0\rangle|^2 = |a\sqrt{1-b^2} - b\sqrt{1-a^2}|^2. \tag{33}$$

Here $b$ is typically small, so that the main contribution comes from the first term. However, the second term is not negligible, and the larger $|b|$ is, the more the weight of the satellite is reduced. A large value of $|b|$ corresponds to a strong coupling between the $\mathrm{d}^9$ and $\mathrm{d}^{10}$ configurations. First we consider the integrated weight

$$\sum_\nu \int_{-\infty}^{0} |V_\nu(\varepsilon)|^2 \,\mathrm{d}\varepsilon \tag{34}$$

of the hopping matrix elements over the valence band and summed over all symmetries. The integration goes to the top $\varepsilon_v = 0$ of the valence band. This quantity is 15 $\mathrm{eV}^2$ for $Cu_2O$ and 21 $\mathrm{eV}^2$ for CuO. For the conduction band the corresponding quantity is 130 and 180 $\mathrm{eV}^2$ for $Cu_2O$ and CuO, respectively. Thus the coupling is generally stronger for CuO than for $Cu_2O$. This means that the larger Cu–O distance in CuO is compensated by the presence of twice as many O neighbours compared with $Cu_2O$. The magnitude of the hopping matrix elements themselves cannot therefore explain the difference between CuO and $Cu_2O$.

We now want to include the effects of the valence of Cu in the two cases, i.e. that the important hopping for $Cu_2O$ is between states a and b in figure 1(*a*) (3d electrons hop into the conduction band) and for CuO between the states a and c in figure 1(*b*) (valence electron hops into the $x^2-y^2$ 3d level). For the final states there is a large separation ( $U_c \sim 10$ eV) between the $\mathrm{d}^9$ and $\mathrm{d}^{10}$ states and the two-level model discussed earlier should be a good approximation. We can define an effective interaction between these two levels, by taking into account an appropriate weighting of the different conduction or valence states. For $Cu_2O$ we introduce

$$V^2_{Cu_2O} = \sum_\nu \int_{E_g}^{\infty} \mathrm{d}E \, \frac{|V_\nu(E)|^2 (U_c - \varepsilon_d + E_g)^2}{(U_c - \varepsilon_d + E)^2} \tag{35}$$

and

$$V^2_{Cu_2O,z^2} = \int_{E_g}^{\infty} \mathrm{d}E \, \frac{|V_{z^2}(E)|^2 (U_c - \varepsilon_d + E_g)^2}{(U_c - \varepsilon_d + E)^2} \tag{36}$$

where $E_g$ is the band gap. Here we have integrated over all conduction states and weighted the contribution with the energy separation between the $\mathrm{d}^{10}$ configuration and the $\mathrm{d}^9$ configuration with a conduction electron with the energy $E$. The result is multiplied by the corresponding energy separation for a two-level model, where we have put the conduction electron at the lowest energy $E_g$. We consider both the total coupling to all symmetries appropriate for $Cu_2O$ and the coupling to the dominating symmetry $z^2$. We obtain the results $V^2_{Cu_2O} = 25$ $\mathrm{eV}^2$ and $V^2_{Cu_2O,z^2} = 5.5$ $\mathrm{eV}^2$.

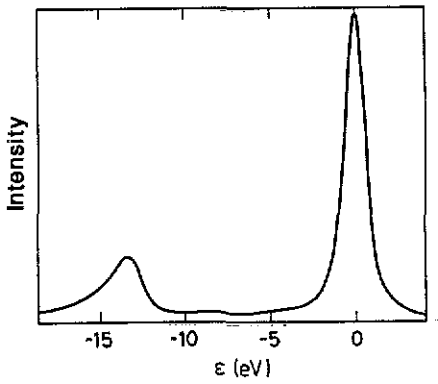


**Figure 6.** Spectrum for $Cu_2O$ with the 3d level raised by 2.6 eV so that the 3d occupancy becomes the same as for CuO.

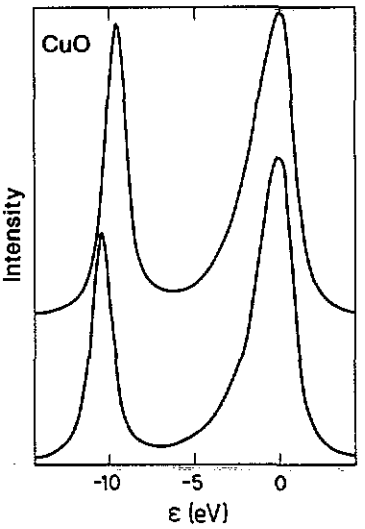


**Figure 7.** The CuO spectrum assuming that the hopping matrix elements are the same in the initial and final state (bottom curve) and that they are reduced by a factor 0.75 in the final state (top curve).

Due to the fact that the coupling is to all symmetries, the effective coupling has been enhanced with a factor $V^2_{Cu_2O}/V^2_{Cu_2O,z^2} = 4.5$, which can be considered as an effective degeneracy. For CuO the hopping from the valence band is important. Since the important valence states occur over a fairly small energy region, we have simply weighted all these states equally. The result is then $V_{CuO}, x^2 - y^2 = 11.9$ eV$^2$. In this case the hopping can only take place in the $x^2 - y^2$ channel.

We now use the two-level model together with these hopping matrix elements. The initial state weights are obtained from the full calculation. We can then calculate the ratio between the weights of the satellite and the main peak. The results are 0.20 and 0.61 for $Cu_2O$ and CuO, in good agreement with the results 0.19 and 0.52 from the full calculation. To separate the different reasons for the smaller satellite in $Cu_2O$, we now perform a calculation for $Cu_2O$, where we replace the proper initial state weights by the weights for CuO. The weight of the satellite relative to the main peak is then predicted to be 0.46. This can be compared with the results in figure 6, where we have raised the 3d level 2.6 eV so that the number of 3d electrons becomes identical to the result for CuO. The weight of the satellite is then increased to 0.38 in good agreement with the two-level calculation. This illustrates that the weight of the satellite in $Cu_2O$ is reduced both because the weight of the $3d^9$ configuration is reduced in the initial state and because there is a stronger coupling in the final state. The stronger coupling in the final state is due to the degeneracy effect discussed earlier, and without this degeneracy effect the coupling would be weaker for $Cu_2O$. Comparison of Figures 3 and 6 also illustrates that the satellite in addition appears very much reduced in $Cu_2O$ because it is strongly broadened in $Cu_2O$, while in CuO the main peak is broadened.

Figure 3 illustrates that the satellite is smaller for $NaCuO_2$ than for CuO. The

coupling between the $d^9$ and $d^{10}$ configurations has a similar structure for $NaCuO_2$ and CuO, and the main difference is therefore the magnitude of the matrix elements. This is illustrated by integrating the most important matrix elements $|V_{x^2-y^2}|^2$ over the valence band. This gives the strength 11.9 $eV^2$ for CuO, as mentioned earlier, and 21.3 $eV^2$ for $NaCuO_2$. In both CuO and $NaCuO_2$, Cu has four nearest-neighbour O atoms. But the Cu–O separation is very small in $NaCuO_2$ (1.85 Å), as is expected for a trivalent compound (more antibonding states emptied), and therefore the coupling is stronger for $NaCuO_2$ than for CuO with a larger Cu–O separation (1.95 Å). This explains why the satellite is much weaker for $NaCuO_2$ than for CuO.

Finally, we discuss the effects of the configuration dependence for the matrix elements, which means that the matrix elements are reduced in the presence of a core hole [11]. The top of figure 7 shows the results when the hopping matrix elements are reduced by a factor 0.75 in the final state, while in the bottom part they are the same in the initial and final state. Due to the more efficient coupling in the bottom part of the figure, the satellite is reduced substantially. The main peak is also narrower. To obtain a reasonable weight for the satellite with equal matrix elements in the initial and final states, one has to raise the 3d level further relative to the calculated value of $\varepsilon_d$ and use $\varepsilon_d = 2.1$ eV. The dependence of the hopping matrix elements on the presence of a core hole has been included in the earlier calculations. The quoted values for $\int |V(\varepsilon)|^2 \, d\varepsilon$ refer to the initial state.

## 4. Summary

We have studied the 2p core level spectra of $Cu_2O$, CuO and $NaCuO_2$, where Cu is monovalent, divalent and trivalent, respectively. In particular we have focused on the weight of the $d^9$ satellite and the width of the main peak. Due to electron counting arguments, the main hopping for the monovalent $Cu_2O$ is between the $d^{10}$ configuration and the $d^9$ configuration with a conduction electron (see states a and b in figure 1(*a*)), while for the divalent CuO the main hopping is between the $d^9$ configuration and the $d^{10}$ configuration with a valence hole (see states a and c in figure 1(*b*)). The large width of the main ($d^{10}$) peak in CuO is due to the presence of a valence hole in the final $d^{10}$ state, where the spread in energy of the hole leads to the width. The same arguments suggest a broad peak also for $NaCuO_2$. In this case, however, the matrix elements are very peaked at the top of the valence band, resulting in a small spread in energy of the holes in the $d^{10}$ states and therefore a small width. For $Cu_2O$ there is a conduction electron present in the $d^9$ configuration, and the $d^9$-like satellite therefore has a substantial broadening for $Cu_2O$ due to the energy spread of the conduction electron.

The difference between $Cu_2O$ and CuO in terms of the weight of the $d^9$ satellite is partly due to the somewhat larger 3d occupancy in $Cu_2O$ ($n_d = 9.42$) than in CuO ($n_d = 9.25$), which favours a larger main ($d^{10}$) peak in $Cu_2O$ and partly due to the stronger coupling in the final states for $Cu_2O$. Since the main coupling in $Cu_2O$ is due to a 3d electron hopping into a conduction state (see states a and b in figure 1(*a*)), the electron can have any quantum number and the coupling is very efficient. In CuO, on the other hand, the main coupling is due to a valence electron hopping into a 3d hole (see states a and c in figure 1(*b*)). Since the quantum number of the 3d hole is fixed ($x^2-y^2$), the hopping can only take place for one specific value of the quantum number of the valence electron. As a result the coupling is weaker

for CuO, and the transfer of weight from the satellite to the main peak is smaller. In addition, the large broadening of the satellite for $Cu_2O$ makes it appear weaker than it is. For $NaCuO_2$ the structure of the hopping matrix element between the $d^9$ and $d^{10}$ configurations is similar as for CuO. The distance to the nearest neighbour O atoms is, however, smaller for the trivalent $NaCuO_2$, and the coupling therefore stronger. This leads to a larger transfer of weight to the main peak and a smaller satellite than for CuO.

## Acknowledgments

We want to thank S Hüfner, J C Fuggle, G A Sawatzky, P Adler and A Simon for useful discussions.

## References

[1] Kotani A and Toyozawa Y 1973 *J. Phys. Soc. Japan* **35** 1073; 1974 *J. Phys. Soc. Japan* **37** 912
[2] Karlsson K, Gunnarsson O and Jepsen O 1992 *J. Phys.: Condens. Matter* **4** 895
[3] Steiner P, Kinsinger V, Sander I, Siegwart B, Hüfner S, Politis C, Hoppe R and Müller H P 1987 *Z. Phys.* B **67** 497
[4] van der Laan G, Westra C, Haas C and Sawatzky G A 1981 *Phys. Rev.* B **23** 4369
[5] Ghijsen J, Tjeng L H, van Elp J, Eskes H, Westerink J, Sawatzky G A and Czyzyk M T 1988 *Phys. Rev.* **38** 11322
Fujimori A, Takayama-Muromachi E, Uchida U and Okai B 1987 *Phys. Rev.* B **35** 8814
Okada K and Kotani A 1990 *J. Electr. Spect. Rel. Phen.* **52** 313
[6] Gunnarsson V and Schönhammer K 1983 *Phys. Rev.* B **28** 4315; 1983 *Phys. Rev. Lett.* **50** 604
[7] Gunnarsson O and Schönhammer K 1987 *Handbook on the Physics and Chemistry of Rare Earths* vol 10, ed K A Gschneider Jr, L Eyring and S Hüfner (Amsterdam: Elsevier) p 103
[8] Hohenberg P and Kohn W 1964 *Phys. Rev.* B **136** 864
Kohn W and Sham L J 1965 *Phys. Rev.* A **140** 1133
[9] Jones R O and Gunnarsson O 1989 *Rev. Mod. Phys.* **61** 689
[10] Gunnarsson O, Andersen O K, Jepsen O and Zaanen J 1989 *Phys. Rev.* B **39** 1708
[11] Gunnarsson O and Jepsen O 1988 *Phys. Rev.* B **38** 3568
[12] Slater J C 1974 *Quantum Theory of Molecules and Solids* vol 4 (New York: McGraw-Hill)
Janak J F 1978 *Phys. Rev.* B **18** 7165
[13] Annett J F, Martin R M, McMahan A K and Satpathy S 1989 *Phys. Rev.* B **40** 2620
[14] Gunnarsson O, Jepsen O and Shen Z-X 1990 *Phys. Rev.* B **42** 8707
[15] Fuggle J C and Alvarado S F 1988 *Phys. Rev.* A **22** 1615
[16] Forsyth J B, Brown P J and Wanklyn B M 1988 *J. Phys. C: Solid State Phys.* **21** 2917
[17] Svane A and Gunnarsson O 1990 *Phys. Rev. Lett.* **65** 1148